

Electron EDM as a Sensitive Probe of PeV Scale Physics

Tarek Ibrahim^{a,b1}, Ahmad Itani^{c2}, and Pran Nath^{d3}

^a Department of Physics, Faculty of Science, University of Alexandria, Alexandria 21511, Egypt⁴

^b Center for Fundamental Physics, Zewail City of Science and Technology, Giza 12588, Egypt⁵

^c Department of Physics, Faculty of Sciences, Beirut Arab University, Beirut 11 - 5020, Lebanon

^d Department of Physics, Northeastern University, Boston, Massachusetts 02115-5000, USA

Abstract

We give a quantitative analysis of the electric dipole moments as a probe of high scale physics. We focus on the electric dipole moment of the electron since the limit on it is the most stringent. Further, theoretical computations of it are free of QCD uncertainties. The analysis presented here first explores the probe of high scales via electron electric dipole moment (EDM) within MSSM where the contributions to the EDM arise from the chargino and the neutralino exchanges in loops. Here it is shown that the electron EDM can probe mass scales from tens of TeV into the PeV range. The analysis is then extended to include a vectorlike generation which can mix with the three ordinary generations. Here new CP phases arise and it is shown that the electron EDM now has not only a supersymmetric contribution from the exchange of charginos and neutralinos but also a non-supersymmetric contribution from the exchange of W and Z bosons. It is further shown that the interference of the supersymmetric and the non-supersymmetric contribution leads to the remarkable phenomenon where the electron EDM as a function of the slepton mass first falls and become vanishingly small and then rises again as the slepton mass increases. This phenomenon arises as a consequence of cancellation between the SUSY and the non-SUSY contribution at low scales while at high scales the SUSY contribution dies out and the EDM is controlled by the non-SUSY contribution alone. The high mass scales that can be probed by the EDM are far in excess of what accelerators will be able to probe. The sensitivity of the EDM to CP phases both in the SUSY and the non-SUSY sectors are also discussed.

Keywords: Electric dipole moments, supersymmetry, PeV scale physics, vector lepton multiplets,

PACS numbers: 13.40Em, 12.60.-i, 14.60.Fg

¹Email: tbrahim@zewailcity.edu.eg

²Email: a.itanis@bau.edu.lb

³Email: nath@neu.edu

⁴Permanent address.

⁵Current address.

1 Introduction

In the standard model the electric dipole moments of elementary particles are very small[1]. Thus for the electron it is estimated that $|d_e| \simeq 10^{-38}$ ecm and for the neutron the value ranges from $10^{-31} - 10^{-33}$ ecm. This is far beyond the current sensitivity of experiments to measure. However, in models of physics beyond the standard model much larger electric dipole moments, orders of magnitude larger than those in the standard model, can be obtained (for a review see [2]). Thus in the supersymmetric models the electric dipole moments of elementary particles such as the electron and the quarks can be large enough that the current experimental upper limits act as constraints on models. Indeed often in supersymmetric theories for light scalars, the electric dipole moments can lie in the region larger than the current upper limits for the electron and the neutron EDMs. This phenomenon is often referred to as the SUSY EDM problem. One solution to the SUSY EDM problem is the possibility that the CP phases are small [3]. Other possibilities allow for large, even maximal, phases and the EDM is suppressed via the sparticle masses being large [4] or by invoking the so called cancellation mechanism [5] where contributions from various diagrams that generate the electric dipole moment interfere destructively to reduce the electric dipole moment to a level below its experimental upper limit.

In the post Higgs boson discovery era the apparent SUSY EDM problem can be turned around to ones advantage as a tool to investigate high scale physics. The logic of this approach is the following: The high mass of the Higgs boson at 126 GeV requires a large loop correction to lift its value from the tree level, which lies below the Z -boson mass, up to the experimental value. A large loop correction requires that the scalar masses that enter in the Higgs boson loop be large so as to generate the desired large correction which requires a high scale for the sfermion masses. Large sfermions masses help with suppression of flavor changing neutral currents. They also help resolve the SUSY EDM problem and help stabilize the proton against decay via baryon and lepton number violating dimension five operators in supersymmetric grand unified theories.

In this work we investigate the possibility that EDMs can be used as probes of high scale physics as suggested in [6, 7, 8, 9]. Specifically we focus here on the EDM of the electron since it is by far the most sensitively determined one than any of the other EDMs. Thus the ACME Collaboration [10] using the polar molecule thorium monoxide (ThO) measures the electron EDM

so that

$$d_e = (-2.1 \pm 3.7_{\text{stat}} \pm 2.5_{\text{syst}}) \times 10^{-29} \text{ ecm}. \quad (1)$$

The above corresponds to an upper limit of

$$|d_e| < 8.7 \times 10^{-29} \text{ ecm} , \quad (2)$$

at 90% CL. The corresponding upper limits on the EDM of the muon and on the tau lepton are [11]

$$|d_\mu| < 1.9 \times 10^{-19} \text{ ecm} , \quad (3)$$

$$|d_\tau| < 10^{-17} \text{ ecm} , \quad (4)$$

and are not as stringent as the result of Eq. (2) even after scaling in lepton mass is taken into account. Further, the limit on d_e is likely to improve by an order of magnitude or more in the future as the projections below indicate

$$\text{Fr}[12] \quad |d_e| \lesssim 1 \times 10^{-29} \text{ ecm} \quad (5)$$

$$\text{YbF molecule}[13] \quad |d_e| \lesssim 1 \times 10^{-30} \text{ ecm} \quad (6)$$

$$\text{WN ion}[14] \quad |d_e| \lesssim 1 \times 10^{-30} \text{ ecm} \quad (7)$$

In the analysis here we will first consider the case of MSSM where the CP phases enter in the soft parameters such as in the masses M_i ($i=1,2$) of the electroweak gauginos, and in the trilinear couplings A_k and in the Higgs mixing parameter μ . Here we will investigate the scale of the slepton masses needed to reduce the electron EDM below its upper limit for the case when the CP phases are naturally $\mathcal{O}(1)$. We will see that this scale will be typically high lying in the range of tens of TeV to a PeV (For a discussion of PeV scale in the context of supersymmetry in previous works see, e.g., [15]). We will carry out the analysis for the case where we extend MSSM to include a vector like leptonic multiplet and allow for mixings between the vector like multiplet and the three sequential generations. We will study the parametric dependence of the EDM on the scalar masses, on fermion masses of the vector like generation, on CP phases and on $\tan \beta$.

The outline of the rest of the paper is as follows: In Section 2 we discuss the EDM of the electron within MSSM as a probe of the slepton masses. In Section 3 we extend the analysis of Section 2 to

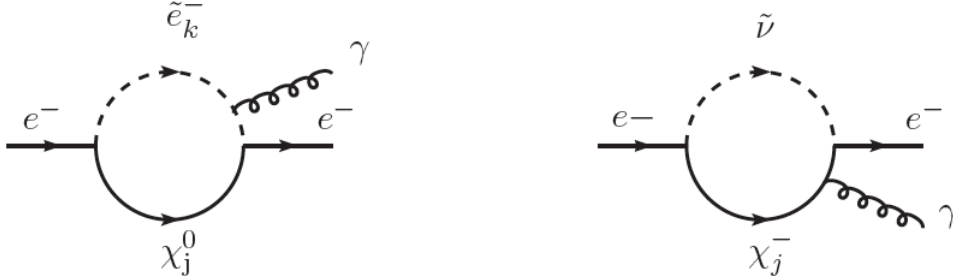


Figure 1: The neutralino-slepton exchange diagram (left) and the chargino-sneutrino exchange diagram (right) that contribute to the electric dipole moment of the electron in MSSM.

MSSM with inclusion of a vector like leptonic multiplet which allows for mixing between the vector multiplet and the three sequential generations. Here we give analytic results for the electron EDM arising from the supersymmetric exchange involving the chargino and neutralinos in the loops. We also compute the non-supersymmetric contributions involving the W and the Z exchange. In Section 4 we give a numerical analysis of the limits on the mass scales that can be accessed using the results of Section 3. Conclusions are given in Section 5. Further details of the MSSM model with a vector multiplet used in the analysis of Section 3 are given in Appendices A-C.

2 Probe of slepton masses in MSSM from the electron EDM constraint

The supersymmetric Feynman diagrams that contribute to the electric dipole moment of the electron involve the chargino-sneutrino exchange and the neutralino-slepton exchange as shown in Fig. 1. In the analysis of these diagrams the input supersymmetry parameters consist of the following

$$M_{\tilde{e}_L}, M_{\tilde{\nu}_e}, M_{\tilde{e}}, \mu, \tan \beta, M_1, M_2, A_e, A_{\nu_e} \quad (8)$$

where $M_{\tilde{e}_L}$ etc are the soft scalar masses, M_1, M_2 are the gaugino masses in the $U(1)$ and $SU(2)$ sectors, A_e etc are the trilinear couplings, μ is the Higgs mixing parameter which enters the superpotential as $\mu H_1 H_2$, where H_2 gives mass to the up quarks and H_1 gives mass to the down quarks and the leptons, while $\tan \beta$ is the ratio of the Higgs VEVs so that $\tan \beta = \langle H_2 \rangle / \langle H_1 \rangle$ (see Appendix A for discussion of the soft parameters). Further, μ, M_1, M_2 , and the trilinear coupling

A_k are complex and we define their phase so that

$$\mu = |\mu|e^{i\alpha\mu}, \quad M_i = |M_i|e^{i\alpha_i}, \quad i = 1, 2 \quad (9)$$

$$A_k = |A_k|e^{i\alpha_{A_k}}, \quad k = e, \nu_e. \quad (10)$$

The analysis of the diagrams of Fig. 1 involves electron-chargino-sneutrino interactions and the electron-neutralino-slepton interactions. For the chargino-sneutrino exchange diagrams one has

$$d_e^{\tilde{\chi}^-} = \frac{\alpha_{em}}{4\pi \sin^2 \theta_W} \frac{k_e}{m_{\tilde{\nu}_e}^2} \sum_{i=1}^2 m_{\tilde{\chi}_i^-} \text{Im}(U_{i2}^* V_{i1}^*) F\left(\frac{m_{\tilde{\chi}_i^-}^2}{m_{\tilde{\nu}_e}^2}\right) \quad (11)$$

where $F(x)$ is a form factor defined by

$$F(x) = \frac{1}{2(1-x)^2} \left(3 - x + \frac{2 \ln x}{1-x} \right) \quad (12)$$

and

$$\kappa_e = \frac{m_e}{\sqrt{2} m_W \cos \beta}. \quad (13)$$

Here U, V diagonalize the chargino mass matrix M_C so that

$$U^* M_C V = \text{diag}(m_{\tilde{\chi}_1^-}, m_{\tilde{\chi}_2^-}). \quad (14)$$

For the neutralino-slepton exchange diagrams one finds

$$d_e^{\tilde{\chi}^0} = \frac{\alpha_{em}}{4\pi \sin^2 \theta_W} \sum_{k=1}^2 \sum_{i=1}^4 \text{Im}(\eta_{eik}) \frac{m_{\tilde{\chi}_i^0}}{M_{\tilde{f}k^2}} Q_{\tilde{f}} G\left(\frac{m_{\tilde{\chi}_i^0}^2}{m_{\tilde{\nu}_e}^2}\right) \quad (15)$$

where $G(x)$ is a form factor defined by

$$G(x) = \frac{1}{2(1-x)^2} \left(1 + x + \frac{2x \ln x}{1-x} \right) \quad (16)$$

where

$$\eta_{eik} = \left[-\sqrt{2} \{ \tan \theta_W (Q_e - T_{3e}) X_{1i} + T_{3i} X_{2i} \} D_{e1k}^* + \kappa_e X_{bi} D_{e2k}^* \right] \quad (17)$$

$$\left(\sqrt{2} \tan \theta_W Q_e X_{1i} D_{e2k} - \kappa_e X_{bi} D_{e1k} \right). \quad (18)$$

where $b = 3$ and $T_{3e} = -1/2$. Further, X_{ij} are elements of the matrix X which diagonalizes the neutralino mass matrix $M_{\tilde{\chi}^0}$ so that

$$X^T M_{\tilde{\chi}^0} X = \text{diag} \left(m_{\tilde{\chi}_1^0}, m_{\tilde{\chi}_2^0}, m_{\tilde{\chi}_3^0}, m_{\tilde{\chi}_4^0} \right), \quad (19)$$

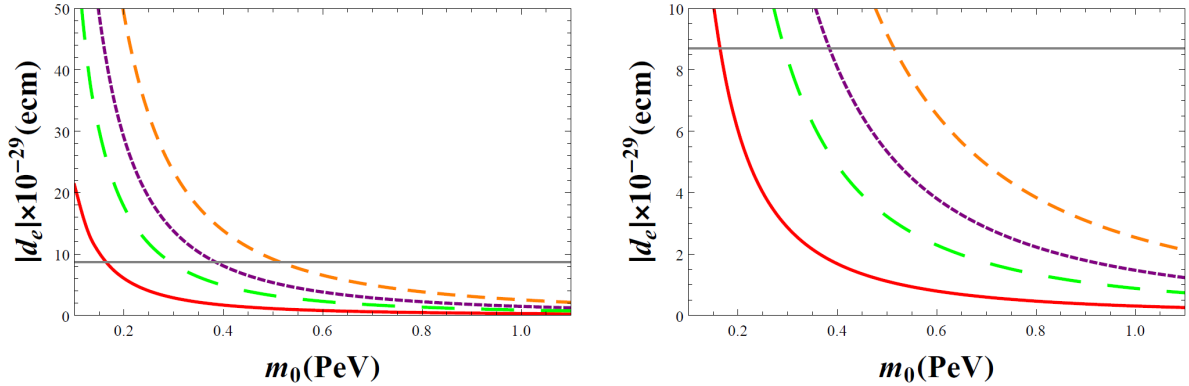


Figure 2: Left panel: A display of the electron EDM as a function of m_0 (where $m_0 = M_{\tilde{e}L} = M_{\tilde{e}}$) for different α_μ (the phase of the Higgs mixing parameter μ) with the mixings of the vector like generation with the regular three generations set to zero. The curves are for the cases $\alpha_\mu = -3$ (small-dashed, red), $\alpha_\mu = -0.5$ (solid), $\alpha_\mu = 1$ (medium-dashed, orange), and $\alpha_\mu = 2.5$ (long-dashed, green). The horizontal solid line is the current upper limit on the electron EDM set at $|d_e| = 8.7 \times 10^{-29}$. The other parameters are $|\mu| = 4.1 \times 10^2$, $|M_1| = 2.8 \times 10^2$, $|M_2| = 3.4 \times 10^2$, $|A_e| = 3 \times 10^6$, $m_{\tilde{0}} = 4 \times 10^6$, $|A_{\tilde{0}}| = 5 \times 10^6$, $\tan\beta = 30$. All masses are in GeV, phases in rad and EDM in ecm. The analysis shows that improvements in the electron EDM constraint can probe scalar masses in the 100 TeV- 1 PeV region and beyond. Right panel: The same as the left panel except that the region below the current experiment limit is blown up. The analysis shows that an improvement by a factor of ten can allow one to probe up to and beyond 1 PeV in mass scales.

and D_e diagonalizes the scalar electron mass ² matrix so that

$$\tilde{e}_L = D_{e11}\tilde{e}_1 + D_{e12}\tilde{e}_2, \quad \tilde{e}_R = D_{e21}\tilde{e}_1 + D_{e22}\tilde{e}_2 \quad (20)$$

where \tilde{e}_1 and \tilde{e}_2 are the selectron mass eigenstates. In Fig. 2 we give a numerical analysis of the electron EDM as a function of m_0 . Here one finds that the current constraint on the electron EDM allows one to probe the m_0 region in the tens of TeV while improvement in the sensitivity by a factor of 10 or more will allow one to extend the range up to 100 TeV - 1 PeV.

3 EDM Analysis by inclusion of a vector generation in MSSM

Next we discuss the case when we include a vectorlike leptonic multiplet which mixes with the three generations of leptons. In this case the mass eigenstates will be linear combinations of the three generations plus the vector like generation which includes mirror particles. The details of the model and its interactions are given in Appendices A-C. Here we discuss the contribution of the

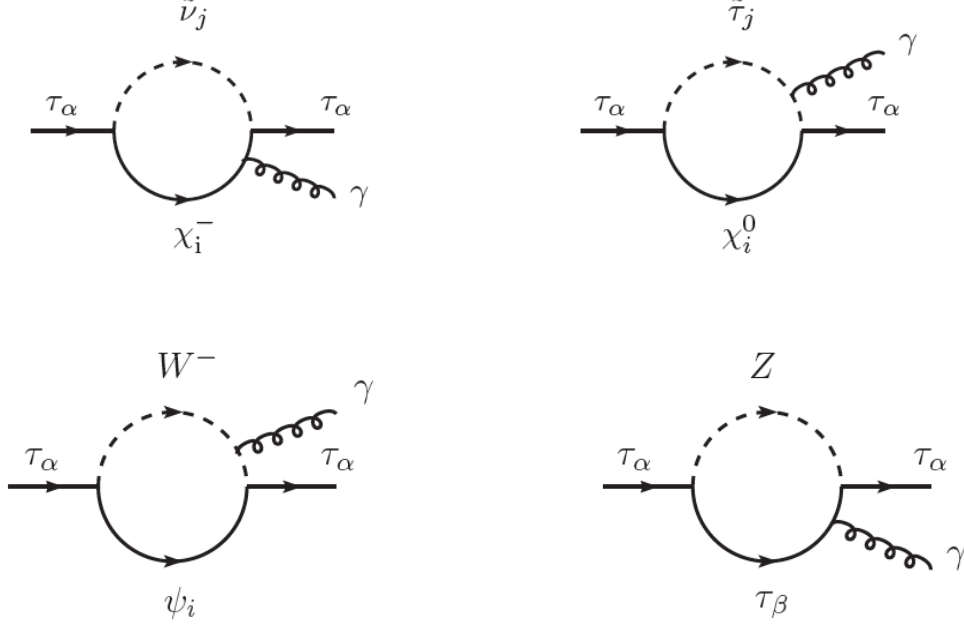


Figure 3: Upper diagrams: Supersymmetric contributions to the leptonic EDMs arising from the exchange of the charginos, sneutrinos and mirror sneutrinos (upper left) and the exchange of neutralinos, sleptons, and mirror sleptons (upper right) inside the loop. Lower diagrams: Non-supersymmetric diagrams that contribute to the leptonic EDMs via the exchange of the W , the sequential and vector like neutrinos (lower left) and the exchange of the Z , the sequential and vector like charged leptons (lower right).

model to the electron EDM. These contributions arise from four sources: the chargino exchange, the neutralino exchange, the W boson exchange and the Z boson exchange.

Using the interactions given in Appendix B the chargino contribution is given by

$$d_\alpha^{\chi^+} = -\frac{1}{16\pi^2} \sum_{i=1}^2 \sum_{j=1}^8 \frac{m_{\chi_i^+}}{m_{\tilde{\nu}_j}^2} \text{Im}(C_{\alpha ij}^L C_{\alpha ij}^{R*}) F\left(\frac{m_{\chi_i^+}^2}{m_{\tilde{\nu}_j}^2}\right) \quad (21)$$

where the functions C^L and C^R are given in Appendix B and the form factor $F(x)$ is given by Eq. (12). Using the interactions given in Appendix B the neutralino contribution is given by

$$d_\alpha^{\chi^0} = -\frac{1}{16\pi^2} \sum_{i=1}^4 \sum_{j=1}^8 \frac{m_{\chi_i^0}}{m_{\tilde{\tau}_j}^2} \text{Im}(C_{\alpha ij}^L C_{\alpha ij}^{R*}) G\left(\frac{m_{\chi_i^0}^2}{m_{\tilde{\tau}_j}^2}\right) \quad (22)$$

where the functions C'^L and C'^R are defined in Appendix B and the form factor $G(x)$ is given by Eq. (16). The contributions to the lepton electric moment from the W and Z exchange arise from similar loops. Using the interactions given in Appendix B the contribution arising from the W exchange diagram is given by

$$d_\alpha^W = \frac{1}{16\pi^2} \sum_{i=1}^4 \frac{m_{\psi_i^+}}{m_W^2} \text{Im}(C_{Li\alpha}^W C_{Ri\alpha}^{W*}) I_1 \left(\frac{m_{\psi_i}^2}{m_W^2} \right) \quad (23)$$

where the functions C_L^W and C_R^W are given in Appendix B and the form factor I_1 is given by

$$I_1(x) = \frac{2}{(1-x)^2} \left[1 - \frac{11}{4}x + \frac{1}{4}x^2 - \frac{3x^2 \ln x}{2(1-x)} \right] \quad (24)$$

The Z boson exchange diagram contribution is given by

$$d_\alpha^Z = -\frac{1}{16\pi^2} \sum_{\beta=1}^4 \frac{m_{\tau_\beta}}{m_Z^2} \text{Im}(C_{L\alpha\beta}^Z C_{R\alpha\beta}^{Z*}) I_2 \left(\frac{m_{\tau_\beta}^2}{m_Z^2} \right) \quad (25)$$

where the functions C_L^Z and C_R^Z are defined in Appendix B and where the form factor I_2 is given by

$$I_2(x) = \frac{2}{(1-x)^2} \left[1 + \frac{1}{4}x + \frac{1}{4}x^2 + \frac{3x \ln x}{2(1-x)} \right] \quad (26)$$

4 Numerical analysis and results

We discuss now the numerical analysis for the EDM of the electron in the model given in Section 3. The parameter space of the model of Section 3 is rather large. In addition to the MSSM parameters, one has the parameters arising from the vectorlike multiplet and its mixings with the standard model generations of quarks and leptons. Thus as in MSSM here also we look at slices of the parameter space to show that interesting new physics exists in these regions. Thus for simplicity in the analysis we assume $A_{\nu_\tau} = A_{\nu_\mu} = A_{\nu_e} = A_N = A_0^{\tilde{\nu}}$ and $m_0^{\tilde{\nu}^2} = M_N^2 = M_{\nu_\tau}^2 = M_{\nu_\mu}^2 = M_{\nu_e}^2$ in the sneutrino mass squared matrix (see Eq. (45)). We also assume $m_0^2 = M_{\tilde{\tau}L}^2 = M_E^2 = M_{\tilde{\tau}}^2 = M_X^2 = M_{\mu L}^2 = M_\mu^2 = M_{eL}^2 = M_e^2$ and $A_0 = A_\tau = A_E = A_\mu = A_e$ in the slepton mass squared matrix (see Eq. (45)). The assumed masses for the new leptons are consistent with the lower limits given by the Particle Data Group[11]. In Fig. 2 we investigated d_e

in MSSM as a function of m_0 when there were no mixing of the ordinary leptonic generations with the vectorlike generation. We wish now to switch on a small mixing with the vector like generation and see what effect it has on the electron EDM. To this end we focus on one curve in Fig. 2 which we take to be the solid curve (the case $\alpha_\mu = -0.5$). For this case we plot the individual contributions to d_e in the left panel of Fig. 4. Here one finds that the largest contribution to d_e arises from the chargino exchange while the neutralino exchange produces a much smaller contribution and as expected the W and Z exchanges do not contribute.

Next we turn on a small coupling between the vector like generation and the three generations of leptons. The analysis for this case is given in the right panel of Fig. 4. The turning on of the mixings has the following effect: the supersymmetric contribution is modified only modestly and its general feature remains as in the left panel. However, now because of mixing with the vectorlike generation the contribution from the W and Z exchange is non-vanishing and in fact is very significant. Further, unlike the chargino and the neutralino exchange contribution the W and Z exchange contribution does not depend on m_0 as exhibited in Fig. 4. Thus as m_0 gets large the supersymmetric contributions becomes much smaller than that of the W and Z exchange contribution. For this reason, d_e is dominated by the W and Z exchange. This phenomenon is exhibited in further detail in Table 1 which is done for the same set of parameters as the right panel of Fig. 4 except that $m_0 = 1.1$ PeV. Here column (i) gives the individual contributions for the case (i) of no mixing where W and Z contributions vanish, and the non-vanishing contributions arise from chargino and neutralino exchange. Column (ii) exhibits the individual contributions when the mixings with the vector like generation are turned on. Here one finds that the supersymmetric contributions from the chargino and neutralino exchanges are essentially unchanged from the case of no mixing but the contributions from the W and Z exchanges are now non-zero and are in fact much larger than the chargino and neutralino exchange contributions. The reason for the non-vanishing contribution from the W and Z exchanges is due to the mixings with vector like generation whose couplings are complex and carry CP violating phases.

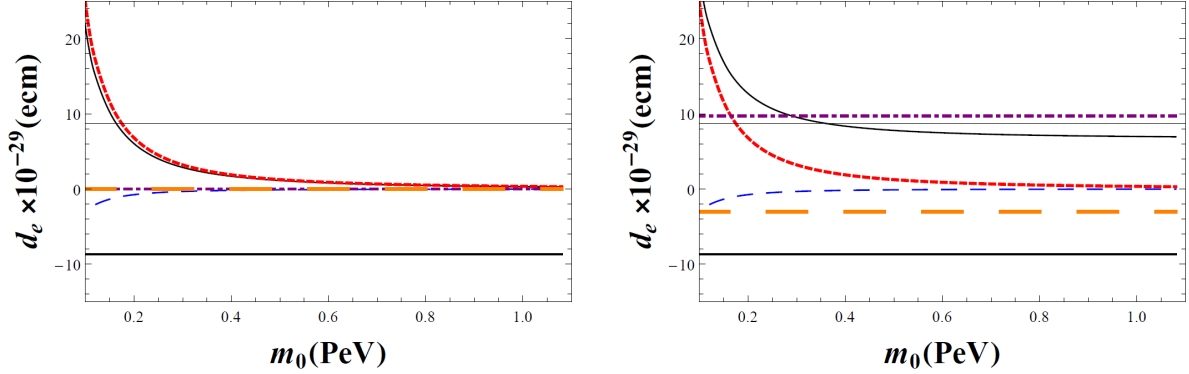


Figure 4: Left Panel: Exhibition of the individual contributions to the EDM of the electron when there is no mixing between the vectorlike generation and the three regular generations. The parameters chosen for this case are the same as for the solid curve in Fig. 2 where $\alpha_\mu = -0.5$. As expected the contributions from the W-exchange (the long-dashed curve in orange) and the Z-exchange (dot-dashed purple curve) give vanishing contribution in this case, and the entire contribution arises from the chargino-exchange (the small-dashed curve in red) and the neutralino-exchange (the medium-dashed blue curve). Right Panel: The parameter point chosen is the same as for the left panel except that mixing of the vectorlike generation with the regular three generations is allowed. The additional parameters chosen are $m_N = 250$, $m_E = 380$ and the f couplings set to $|f_3| = 7.20 \times 10^{-6}$, $|f'_3| = 1.19 \times 10^{-4}$, $|f''_3| = 1.55 \times 10^{-5}$, $|f_4| = 8.13 \times 10^{-4}$, $|f'_4| = 3.50 \times 10^{-1}$, $|f''_4| = 6.29 \times 10^{-1}$, $|f_5| = 8.82 \times 10^{-5}$, $|f'_5| = 5.36 \times 10^{-5}$, $|f''_5| = 1.27 \times 10^{-5}$. Their corresponding CP phases set to $\chi_3 = 9.71 \times 10^{-1}$, $\chi'_3 = 7.86 \times 10^{-1}$, $\chi''_3 = 7.89 \times 10^{-1}$, $\chi_4 = 7.66 \times 10^{-1}$, $\chi'_4 = 8.38 \times 10^{-1}$, $\chi''_4 = 8.23 \times 10^{-1}$, $\chi_5 = 7.70 \times 10^{-1}$, $\chi'_5 = 1.47$, $\chi''_5 = 7.82 \times 10^{-1}$. All masses are in GeV, phases in rad and EDM in ecm.

	(i) Case of no mixing	(ii) Case of mixing
$d_e^{\chi^+}$	2.82×10^{-30}	2.82×10^{-30}
$d_e^{\chi^0}$	-2.53×10^{-31}	-2.53×10^{-31}
d_e^W	0	9.72×10^{-29}
d_e^Z	0	-3.05×10^{-29}
d_e	2.57×10^{-30}	6.93×10^{-29}

Table 1: Column (i): An exhibition of the individual contributions to d_e arising from the chargino, neutralino, W and Z boson exchanges and their sum d_e for the case when there is no mixing among the generations. The parameters chosen are the same as for the solid curve ($\alpha_\mu = -0.5$ rad) of Fig. 2 where m_0 is set to 1.1 PeV. Column (ii): The analysis of column (ii) has the same set of parameters as the left panel except that inter-generational couplings are allowed. Here the couplings $f_3, f'_3, f''_3, f_4, f'_4, f''_4, f_5, f'_5, f''_5$ are the same as the ones in the right panel of Fig. 4. The fermion masses for the vectorlike generation are $m_N = 250$ and $m_E = 380$ GeV. The EDM is in ecm units.

In Fig. 5 we give an analysis of the electron EDM as a function of m_0 for different pairs of fermion masses for the vectorlike generation. The fermion masses for the vectorlike generation lies in the range 150-300 GeV. Here we find that d_e is very sensitive to the fermion masses for the vector like generation. The dependence of $|d_e|$ on m_0 shows a turn around where $|d_e|$ first decreases and then increases. This is easily understood as follows: As discussed already for the case of Fig. 4 the supersymmetric contribution is very sensitive to m_0 since the sleptons that enter in the supersymmetric diagrams get large as m_0 gets large and consequently the SUSY contributions become negligible as m_0 gets large. However, also as already discussed the W and Z exchange contributions are not affected by m_0 . Thus at low values of m_0 , the supersymmetric contribution is large and of opposite sign to the W and Z exchange contribution in this region of the parameter space which leads to a cancellation between the two thus a falling behavior of $|d_e|$. However, as m_0 increases the SUSY contribution dies out and the W and Z contribution take over which explains the turn around. This turn around is exhibited for two values of m_0 around the minimum in Table 2. Here we consider the parameter point $m_N = m_E = 200$ GeV in Fig. 4 for the sample points $m_0 = 0.4$ PeV and $m_0 = 0.6$ PeV. Comparison of columns (i) and (ii) in Table 2 shows that the chargino and the neutralino exchange contribution vary in a significant way while the W and Z exchange contribution is unchanged. Consequently $d_e = -5.96 \times 10^{-29}$ ecm for column (i) and $d_e = 6.61 \times 10^{-29}$ ecm for column (ii). Thus we see that the d_e has switched the sign in going from $m_0 = 0.4$ PeV to $m_0 = 0.6$ PeV which means that d_e has gone through a zero which explains the turn around of $|d_e|$ in Fig. 5.

In Fig. 6 we exhibit the dependence of $|d_e|$ on the phase α_μ which is the phase of the Higgs mixing parameter μ . The dependence of $|d_e|$ on α_μ arises from various sources. Thus the slepton masses as well as the chargino and the neutrino masses that enter in the supersymmetric loop contribution have a dependence on α_μ which makes a simple explanation of the dependence on this parameter less transparent. A numerical analysis exhibiting the dependence of $|d_e|$ on α_μ is given in Fig. 6. The analysis is done for different $\tan\beta$ ranging from $\tan\beta = 20$ to $\tan\beta = 50$. A similar analysis of the dependence of $|d_e|$ on χ_4'' for various values of f_4'' is given in Fig. 7. The sharp dependence of $|d_e|$ on χ_4'' is not difficult to understand. Unlike the case of the dependence of $|d_e|$ on α_μ which arises mainly from the supersymmetric sector, here the dependence of $|d_e|$ on χ_4'' arises from the non-supersymmetric sector via the exchange of W and Z bosons. The SUSY contribution dependence is limited by the smallness of $|f_4''|$ compared to the other masses in the slepton mass² matrix. The non-supersymmetric contribution is directly governed by f_3'', f_4'', f_5'' as

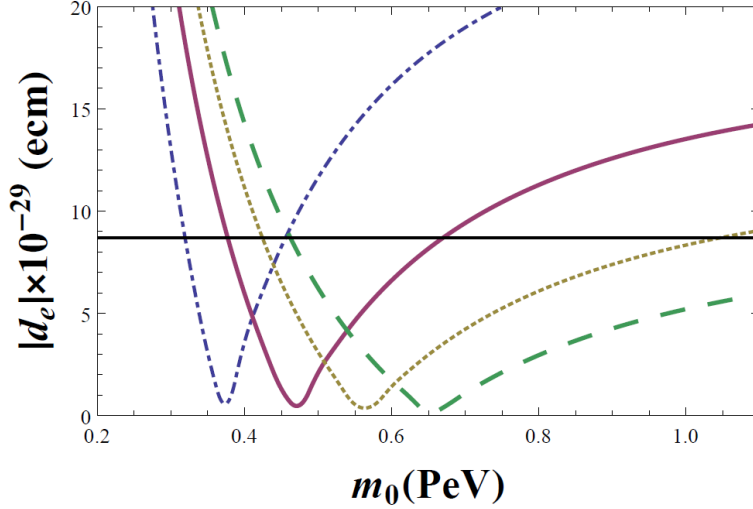


Figure 5: An exhibition of the dependence of $|d_e|$ on m_0 for various vectorlike masses. The curves correspond to $m_N = m_E = 150$ (dotdashed), $m_N = m_E = 200$ (solid), $m_N = m_E = 250$ (dotted), $m_N = m_E = 300$ (dashed). The parameters are $|\mu| = 4.1 \times 10^2$, $|M_1| = 2.8 \times 10^2$, $|M_2| = 3.4 \times 10^2$, $|A_0| = 3 \times 10^6$, $m_0^{\tilde{\nu}} = 4 \times 10^6$, $|A_0^{\tilde{\nu}}| = 5 \times 10^6$, $\tan\beta = 50$. The CP phases are $\theta_\mu = 1$, $\alpha_1 = 1.26$, $\alpha_2 = 0.94$, $\alpha_{A_0} = 0.94$, $\alpha_{A_0^{\tilde{\nu}}} = 1.88$. The f couplings are $|f_3| = 3.01 \times 10^{-5}$, $|f'_3| = 8.07 \times 10^{-6}$, $|f''_3| = 2.06 \times 10^{-5}$, $|f_4| = 8.13 \times 10^{-4}$, $|f'_4| = 3.50 \times 10^{-1}$, $|f''_4| = 6.29 \times 10^{-1}$, $|f_5| = 6.38 \times 10^{-5}$, $|f'_5| = 1.03 \times 10^{-6}$, $|f''_5| = 2.44 \times 10^{-8}$. Their corresponding CP phases are $\chi_3 = 7.91 \times 10^{-1}$, $\chi'_3 = 7.87 \times 10^{-1}$, $\chi''_3 = 7.78 \times 10^{-1}$, $\chi_4 = 7.66 \times 10^{-1}$, $\chi'_4 = 8.38 \times 10^{-1}$, $\chi''_4 = 8.23 \times 10^{-1}$, $\chi_5 = 7.57 \times 10^{-1}$, $\chi'_5 = 7.54 \times 10^{-1}$, $\chi''_5 = 7.83 \times 10^{-1}$. All masses are in GeV, phases in rad, and d_e in ecm.

can be seen from Eq.(36) and Eq.(40). Here setting $f''_3 = f''_4 = f''_5 = 0$ puts the mass matrices in a block diagonal form where the first generation totally decouples from the vector like generation. This clearly indicates that the effect of variation in $|f''_3|, |f''_4|, |f''_5|$ and their phases, $\chi''_3, \chi''_4, \chi''_5$ will be strong. This is what the analysis of Fig. 7 indicates. Aside from the variations of the W and Z contributions on χ''_4 , there is also a constructive/destructive interference between the W and the Z contributions as χ''_4 varies which explains the rapid variations of $|d_e|$ with χ''_4 in Fig. 7.

Finally, the effect of mixing of the vectorlike generation with the three lepton generations has negligible effect on the standard model predictions in the leptonic sector at the tree level. However, it does affect the neutrino sector. Specifically taking the mixings into account the analysis presented here satisfies the constraint on the sum of the neutrino masses arising from the Planck Satellite

experiment [30] so that

$$\sum_{i=1}^3 m_{\nu_i} < 0.85 \text{ eV} , \quad (27)$$

where we assume ν_i ($i=1,2,3$) to be the mass eigenstates with eigenvalues m_{ν_i} . Further, the neutrino oscillations constraint on the neutrino mass squared differences [30] are also satisfied, i.e., the constraints

$$\Delta m_{31}^2 \equiv m_3^2 - m_1^2 = 2.4_{-0.11}^{+0.12} \times 10^{-3} \text{ eV}^2 , \quad (28)$$

$$\Delta m_{21}^2 \equiv m_2^2 - m_1^2 = 7.65_{-0.20}^{+0.23} \times 10^{-5} \text{ eV}^2 . \quad (29)$$

The analysis given in this section respect all of the collider, i.e., LEP and LHC, constraints. Specifically the lower limits on heavy lepton masses is around 100 GeV[11] and masses of m_E and m_N used here respect these limits. However, in addition there are flavor constraints to consider. Here the constraint $\mu \rightarrow e + \gamma$ is the most stringent constraint. Thus the above framework allows the process $\mu \rightarrow e + \gamma$ for which the current upper limit from experiment is [11] 4.4×10^{-12} . The analysis of this process requires the mixing of the vectorlike generation with all the three generations. A similar analysis but for the $\tau \rightarrow \mu + \gamma$ was given in [27] and it was found that the model with a vector like generation can produce a branching ratio for this process which lies below the current experimental limit for that process but could be accessible in improved experiment . In that analysis the scalar masses were in the sub TeV region. However, in the present case we are interested in the PeV size scalar masses. From Figure 3 of [27], we see that for heavy scalars, the branching ratio decreases rapidly as the masses increase and since we are interested in the PeV size scalars we expect that the $\mu \rightarrow e + \gamma$ experimental upper limits would be easily satisfied. A full treatment of the processes is, however, outside the scope of this work and will be discussed elsewhere.

	(i) $m_0 = 0.4$ PeV	(ii) $m_0 = 0.6$ PeV
$d_e^{\chi^+}$	-2.38×10^{-28}	-1.13×10^{-28}
$d_e^{\chi^0}$	-9.18×10^{-31}	-4.08×10^{-31}
d_e^W	2.72×10^{-28}	2.72×10^{-28}
d_e^Z	-9.31×10^{-29}	-9.31×10^{-29}
d_e	-5.96×10^{-29}	6.61×10^{-29}

Table 2: An exhibition of the individual contributions to the electric dipole moment of the electron arising from the chargino exchange, neutralino exchange, W boson exchange and Z boson exchange. The last row gives the total EDM d_e where $d_e = d_e^{\chi^+} + d_e^{\chi^0} + d_e^W + d_e^Z$. The analysis is for the solid curve of Fig. 5 where $m_N = m_E = 200$ when (i) $m_0 = 0.4$ PeV, (ii) $m_0 = 0.6$ PeV. The EDM is in ecm units.

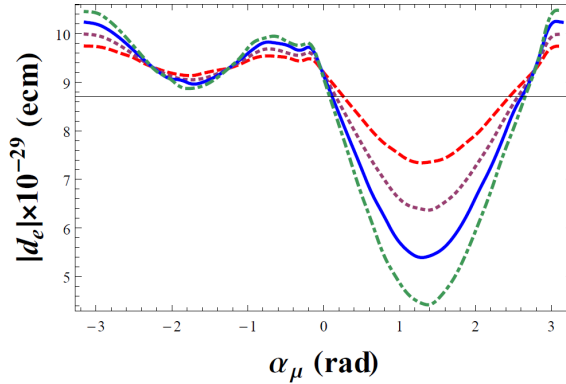


Figure 6: An exhibition of the dependence of $|d_e|$ on α_μ for various $\tan\beta$. The curves correspond to $\tan\beta = 20$ (dashed), $\tan\beta = 30$ (dotted), $\tan\beta = 40$ (solid), and $\tan\beta = 50$ (dotdashed). The parameters used are $|\mu| = 3.9 \times 10^2$, $|M_1| = 3.1 \times 10^2$, $|M_2| = 3.6 \times 10^2$, $m_N = 340$, $m_E = 250$, $m_0 = 1.1 \times 10^6$, $|A_0| = 3.2 \times 10^6$, $m_0^{\tilde{\nu}} = 4.3 \times 10^6$, $|A_0^{\tilde{\nu}}| = 5.1 \times 10^6$, $\alpha_1 = 1.88$, $\alpha_2 = 1.26$, $\alpha_{A_0} = 0.94$, $\alpha_{A_0^{\tilde{\nu}}} = 1.88$. The mixings are $|f_3| = 2.88 \times 10^{-4}$, $|f_3'| = 8.19 \times 10^{-6}$, $|f_3''| = 9.19 \times 10^{-5}$, $|f_4| = 8.13 \times 10^{-4}$, $|f_4'| = 3.50 \times 10^{-1}$, $|f_4''| = 1.29 \times 10^{-1}$, $|f_5| = 5.75 \times 10^{-6}$, $|f_5'| = 1.00 \times 10^{-5}$, $|f_5''| = 2.49 \times 10^{-7}$, $\chi_3 = 7.74 \times 10^{-1}$, $\chi_3' = 7.73 \times 10^{-1}$, $\chi_3'' = 7.86 \times 10^{-1}$, $\chi_4 = 7.6 \times 10^{-1}$, $\chi_4' = 8.40 \times 10^{-1}$, $\chi_4'' = 8.20 \times 10^{-1}$, $\chi_5 = 7.51 \times 10^{-1}$, $\chi_5' = 8.19 \times 10^{-1}$, $\chi_5'' = 8.03 \times 10^{-1}$. All masses are in GeV, phases in rad, and d_e in ecm.

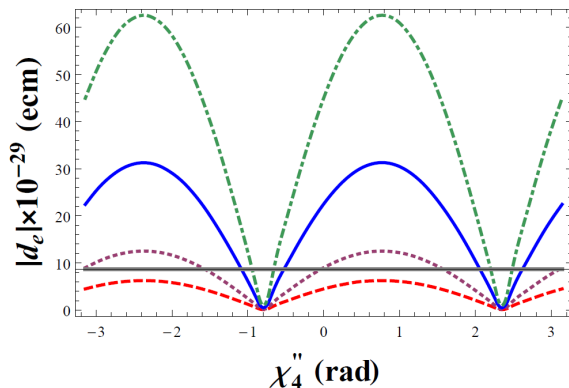


Figure 7: An exhibition of the dependence of $|d_e|$ on χ_4'' for various f_4'' . The curves correspond to f_4'' of 0.1 (dashed), 0.2 (dotted), 0.5 (solid), 1 (dot-dashed). The other parameters are $|\mu| = 1.1 \times 10^6$, $|M_1| = 2.8 \times 10^6$, $|M_2| = 3.4 \times 10^6$, $m_N = 250$, $m_E = 380$, $m_0 = 1.1 \times 10^6$, $|A_0| = 3.2 \times 10^6$, $m_{\tilde{0}} = 1.4 \times 10^6$, $|A_{\tilde{0}}| = 5.1 \times 10^6$, $\alpha_1 = 1.26$, $\alpha_2 = 0.94$, $\alpha_{A_0} = 0.94$, $\alpha_{A_{\tilde{0}}} = 1.88$, $\tan\beta = 30$. The mixings are $|f_3| = 2.93 \times 10^{-4}$, $|f_3'| = 8.19 \times 10^{-6}$, $|f_3''| = 9.15 \times 10^{-5}$, $|f_4| = 8.13 \times 10^{-1}$, $|f_4'| = 3.50 \times 10^{-1}$, $|f_5| = 5.08 \times 10^{-6}$, $|f_5'| = 9.98 \times 10^{-6}$, $|f_5''| = 2.56 \times 10^{-7}$, $\chi_3 = 7.86 \times 10^{-1}$, $\chi_3' = 7.80 \times 10^{-1}$, $\chi_3'' = 8.02 \times 10^{-1}$, $\chi_4 = 7.6 \times 10^{-1}$, $\chi_4' = 8.4 \times 10^{-1}$, $\chi_5 = 7.39 \times 10^{-1}$, $\chi_5' = 7.82 \times 10^{-1}$, $\chi_5'' = 7.82 \times 10^{-1}$. All masses are in GeV, phases in rad and d_e in ecm.

5 Conclusion

In the future the exploration of high scale physics on the energy frontier will be limited by the capability on the highest energy that accelerators can achieve. Thus the upgraded LHC will achieve an energy of $\sqrt{s} = 13$ TeV. Proposals are afoot to build accelerators that could extend the range to an ambitious goal of 100 TeV. It has been pointed out recently that there are other avenues to access high scales and one of these is via sensitive measurement of the EDM of elementary particles, i.e., of leptons and of quarks. In this work we focus on the EDM of the electron as it is the most stringently constrained of the EDMs. In this analysis we have used the current experimental limits on the EDM of the electron to explore in a quantitative fashion the scale of the slepton masses that the electron EDM can explore within MSSM. It is found that the current constraints allow one to explore a wide scale of slepton masses from few TeV to a PeV and beyond. Further, we have extended the analysis to include a vector like lepton generation and allowing for small mixings between the three ordinary generations and the vector like generation. Here in addition to the supersymmetric contribution involving the exchange of the charginos and the neutralinos, one has in addition a contribution arising from the exchange of the W and of the Z bosons. Unlike the chargino and the neutralino

contribution which is sensitive to the slepton masses, the W and Z contribution is independent of them. Thus the interference between the supersymmetric and the non-supersymmetric contribution produces a remarkable phenomenon where the EDM first falls and then turns around and rises again as the common scalar mass m_0 increases. This is easily understood by noting that the destructive interference between the supersymmetric and the non-supersymmetric contribution leads first to a cancellation between the two but as the supersymmetric contribution dies out with increasing m_0 the non-supersymmetric contribution becomes dominant and controls the EDM. Thus in this case EDM could be substantial even when m_0 lies in the several PeV region. In the future, the EDM of the electron will be constrained even more stringently by a factor of ten or more. Such a more stringent constraint will allow one to explore even a larger range in the slepton masses. Finally we note that a large SUSY sfermion scale in the PeV region would automatically relieve the tension on flavor changing neutral current problem and on too rapid a proton decay in supersymmetric grand unified theories [16].

Acknowledgments: This research was supported in part by the NSF Grant PHY-1314774, XSEDE-TG-PHY110015, and NERSC-DE-AC02-05CH1123.

Appendix A: The MSSM Extension with a vector leptonic multiplet

In Section 3 we extended MSSM to include a vector like generation. Here we provide further details of this extension. A vectorlike multiplet consists of an ordinary fourth generation of leptons, quarks and their mirrors. A vector like generation is anomaly free and thus inclusion of it respects the good properties of a gauge theory. Vector like multiplets arise in a variety of unified models [17] some of which could be low lying. They have been used recently in a variety of analyses [18, 19, 20, 21, 22, 23, 24, 25, 26, 28]. In the analysis below we will assume an extended MSSM with just one vector multiplet. Before proceeding further we define the notation and give a very brief description of the extended model and a more detailed description can be found in the previous works mentioned above. Thus the extended MSSM contains a vectorlike multiplet. To fix notation the three generations of leptons are denoted by

$$\psi_{iL} \equiv \begin{pmatrix} \nu_{iL} \\ l_{iL} \end{pmatrix} \sim (1, 2, -\frac{1}{2}) ; \quad l_{iL}^c \sim (1, 1, 1) ; \quad \nu_{iL}^c \sim (1, 1, 0) ; \quad i = 1, 2, 3 \quad (30)$$

where the properties under $SU(3)_C \times SU(2)_L \times U(1)_Y$ are also exhibited. The last entry in the braces such as $(1, 2, -1/2)$ is the value of the hypercharge Y defined so that $Q = T_3 + Y$. These

leptons have $V - A$ interactions. We can now add a vectorlike multiplet where we have a fourth family of leptons with $V - A$ interactions whose transformations can be gotten from Eq.(30) by letting i run from 1 to 4. A vectorlike lepton multiplet also has mirrors and so we consider these mirror leptons which have $V + A$ interactions. The quantum numbers of the mirrors are given by

$$\chi^c \equiv \begin{pmatrix} E_L^c \\ N_L^c \end{pmatrix} \sim (1, 2, \frac{1}{2}) ; \quad E_L \sim (1, 1, -1) ; \quad N_L \sim (1, 1, 0). \quad (31)$$

Interesting new physics arises when we allow mixings of the vectorlike generation with the three ordinary generations. Here we focus on the mixing of the mirrors in the vectorlike generation with the three generations. Thus the superpotential of the model allowing for the mixings among the three ordinary generations and the vectorlike generation is given by

$$\begin{aligned} W = & -\mu\epsilon_{ij}\hat{H}_1^i\hat{H}_2^j + \epsilon_{ij}[f_1\hat{H}_1^i\hat{\psi}_L^j\hat{\tau}_L^c + f'_1\hat{H}_2^j\hat{\psi}_L^i\hat{\nu}_{\tau L}^c + f_2\hat{H}_1^i\hat{\chi}^{cj}\hat{N}_L + f'_2\hat{H}_2^j\hat{\chi}^{ci}\hat{E}_L \\ & + h_1H_1^i\hat{\psi}_{\mu L}^j\hat{\mu}_L^c + h'_1H_2^j\hat{\psi}_{\mu L}^i\hat{\nu}_{\mu L}^c + h_2H_1^i\hat{\psi}_{eL}^j\hat{e}_L^c + h'_2H_2^j\hat{\psi}_{eL}^i\hat{\nu}_{eL}^c] \\ & + f_3\epsilon_{ij}\hat{\chi}^{ci}\hat{\psi}_L^j + f'_3\epsilon_{ij}\hat{\chi}^{ci}\hat{\psi}_{\mu L}^j + f_4\hat{\tau}_L^c\hat{E}_L + f_5\hat{\nu}_{\tau L}^c\hat{N}_L + f'_4\hat{\mu}_L^c\hat{E}_L + f'_5\hat{\nu}_{\mu L}^c\hat{N}_L \\ & + f''_3\epsilon_{ij}\hat{\chi}^{ci}\hat{\psi}_{eL}^j + f''_4\hat{e}_L^c\hat{E}_L + f''_5\hat{\nu}_{eL}^c\hat{N}_L , \end{aligned} \quad (32)$$

where $\hat{}$ implies superfields, $\hat{\psi}_L$ stands for $\hat{\psi}_{3L}$, $\hat{\psi}_{\mu L}$ stands for $\hat{\psi}_{2L}$ and $\hat{\psi}_{eL}$ stands for $\hat{\psi}_{1L}$. The mass terms for the neutrinos, mirror neutrinos, leptons and mirror leptons arise from the term

$$\mathcal{L} = -\frac{1}{2}\frac{\partial^2 W}{\partial A_i \partial A_j}\psi_i\psi_j + \text{H.c.} \quad (33)$$

where ψ and A stand for generic two-component fermion and scalar fields. After spontaneous breaking of the electroweak symmetry, ($\langle H_1^1 \rangle = v_1/\sqrt{2}$ and $\langle H_2^2 \rangle = v_2/\sqrt{2}$), we have the following set of mass terms written in the 4-component spinor notation so that

$$-\mathcal{L}_m = \bar{\xi}_R^T(M_f)\xi_L + \bar{\eta}_R^T(M_\ell)\eta_L + \text{H.c.}, \quad (34)$$

where the basis vectors in which the mass matrix is written is given by

$$\begin{aligned} \bar{\xi}_R^T &= (\bar{\nu}_{\tau R} \quad \bar{N}_R \quad \bar{\nu}_{\mu R} \quad \bar{\nu}_{eR}), \\ \xi_L^T &= (\nu_{\tau L} \quad N_L \quad \nu_{\mu L} \quad \nu_{eL}), \\ \bar{\eta}_R^T &= (\bar{\tau}_R \quad \bar{E}_R \quad \bar{\mu}_R \quad \bar{e}_R), \\ \eta_L^T &= (\tau_L \quad E_L \quad \mu_L \quad e_L), \end{aligned} \quad (35)$$

and the mass matrix M_f is given by

$$M_f = \begin{pmatrix} f'_1 v_2 / \sqrt{2} & f_5 & 0 & 0 \\ -f_3 & f_2 v_1 / \sqrt{2} & -f'_3 & -f''_3 \\ 0 & f'_5 & h'_1 v_2 / \sqrt{2} & 0 \\ 0 & f''_5 & 0 & h'_2 v_2 / \sqrt{2} \end{pmatrix}. \quad (36)$$

We define the matrix element (22) of the mass matrix as m_N so that

$$m_N = f_2 v_1 / \sqrt{2}. \quad (37)$$

The mass matrix is not hermitian and thus one needs bi-unitary transformations to diagonalize it. We define the bi-unitary transformation so that

$$D_R^{\nu\dagger} (M_f) D_L^\nu = \text{diag}(m_{\psi_1}, m_{\psi_2}, m_{\psi_3}, m_{\psi_4}). \quad (38)$$

Under the bi-unitary transformations the basis vectors transform so that

$$\begin{pmatrix} \nu_{\tau R} \\ N_R \\ \nu_{\mu R} \\ \nu_{e R} \end{pmatrix} = D_R^\nu \begin{pmatrix} \psi_{1R} \\ \psi_{2R} \\ \psi_{3R} \\ \psi_{4R} \end{pmatrix}, \quad \begin{pmatrix} \nu_{\tau L} \\ N_L \\ \nu_{\mu L} \\ \nu_{e L} \end{pmatrix} = D_L^\nu \begin{pmatrix} \psi_{1L} \\ \psi_{2L} \\ \psi_{3L} \\ \psi_{4L} \end{pmatrix}. \quad (39)$$

In Eq. (38) $\psi_1, \psi_2, \psi_3, \psi_4$ are the mass eigenstates for the neutrinos, where in the limit of no mixing we identify ψ_1 as the light tau neutrino, ψ_2 as the heavier mass eigen state, ψ_3 as the muon neutrino and ψ_4 as the electron neutrino. A similar analysis goes to the lepton mass matrix M_ℓ where

$$M_\ell = \begin{pmatrix} f_1 v_1 / \sqrt{2} & f_4 & 0 & 0 \\ f_3 & f'_2 v_2 / \sqrt{2} & f'_3 & f''_3 \\ 0 & f'_4 & h_1 v_1 / \sqrt{2} & 0 \\ 0 & f''_4 & 0 & h_2 v_1 / \sqrt{2} \end{pmatrix}. \quad (40)$$

In general $f_3, f_4, f_5, f'_3, f'_4, f'_5, f''_3, f''_4, f''_5$ can be complex and we define their phases so that

$$f_k = |f_k| e^{i\chi_k}, \quad f'_k = |f'_k| e^{i\chi'_k}, \quad f''_k = |f''_k| e^{i\chi''_k}; \quad k = 3, 4, 5. \quad (41)$$

We introduce now the mass parameter m_E defined by the (22) element of the mass matrix above so that

$$m_E = f'_2 v_2 / \sqrt{2}. \quad (42)$$

Next we consider the mixing of the charged sleptons and the charged mirror sleptons. The mass squared matrix of the slepton - mirror slepton comes from three sources: the F term, the D term of the potential and the soft SUSY breaking terms. Using the superpotential of Eq. (32) the mass terms arising from it after the breaking of the electroweak symmetry are given by the Lagrangian

$$\mathcal{L} = \mathcal{L}_F + \mathcal{L}_D + \mathcal{L}_{\text{soft}} , \quad (43)$$

where \mathcal{L}_F is deduced from Eq. (32) and is given in [27], while the \mathcal{L}_D is given by

$$\begin{aligned} -\mathcal{L}_D = & \frac{1}{2}m_Z^2 \cos^2 \theta_W \cos 2\beta \{ \tilde{\nu}_{\tau L} \tilde{\nu}_{\tau L}^* - \tilde{\tau}_L \tilde{\tau}_L^* + \tilde{\nu}_{\mu L} \tilde{\nu}_{\mu L}^* - \tilde{\mu}_L \tilde{\mu}_L^* + \tilde{\nu}_{eL} \tilde{\nu}_{eL}^* - \tilde{e}_L \tilde{e}_L^* \\ & + \tilde{E}_R \tilde{E}_R^* - \tilde{N}_R \tilde{N}_R^* \} + \frac{1}{2}m_Z^2 \sin^2 \theta_W \cos 2\beta \{ \tilde{\nu}_{\tau L} \tilde{\nu}_{\tau L}^* + \tilde{\tau}_L \tilde{\tau}_L^* + \tilde{\nu}_{\mu L} \tilde{\nu}_{\mu L}^* + \tilde{\mu}_L \tilde{\mu}_L^* \\ & + \tilde{\nu}_{eL} \tilde{\nu}_{eL}^* + \tilde{e}_L \tilde{e}_L^* - \tilde{E}_R \tilde{E}_R^* - \tilde{N}_R \tilde{N}_R^* + 2\tilde{E}_L \tilde{E}_L^* - 2\tilde{\tau}_R \tilde{\tau}_R^* - 2\tilde{\mu}_R \tilde{\mu}_R^* - 2\tilde{e}_R \tilde{e}_R^* \} . \end{aligned} \quad (44)$$

For $\mathcal{L}_{\text{soft}}$ we assume the following form

$$\begin{aligned} -\mathcal{L}_{\text{soft}} = & M_{\tilde{\tau}L}^2 \tilde{\psi}_{\tau L}^{i*} \tilde{\psi}_{\tau L}^i + M_{\tilde{\chi}}^2 \tilde{\chi}^{ci*} \tilde{\chi}^{ci} + M_{\tilde{\mu}L}^2 \tilde{\psi}_{\mu L}^{i*} \tilde{\psi}_{\mu L}^i + M_{\tilde{e}L}^2 \tilde{\psi}_{eL}^{i*} \tilde{\psi}_{eL}^i + M_{\tilde{\nu}_\tau}^2 \tilde{\nu}_{\tau L}^{c*} \tilde{\nu}_{\tau L}^c + M_{\tilde{\nu}_\mu}^2 \tilde{\nu}_{\mu L}^{c*} \tilde{\nu}_{\mu L}^c \\ & + M_{\tilde{\nu}_e}^2 \tilde{\nu}_{eL}^{c*} \tilde{\nu}_{eL}^c + M_{\tilde{\tau}}^2 \tilde{\tau}_L^{c*} \tilde{\tau}_L^c + M_{\tilde{\mu}}^2 \tilde{\mu}_L^{c*} \tilde{\mu}_L^c + M_{\tilde{e}}^2 \tilde{e}_L^{c*} \tilde{e}_L^c + M_{\tilde{E}}^2 \tilde{E}_L^* \tilde{E}_L + M_{\tilde{N}}^2 \tilde{N}_L^* \tilde{N}_L \\ & + \epsilon_{ij} \{ f_1 A_\tau H_1^i \tilde{\psi}_{\tau L}^j \tilde{\tau}_L^c - f'_1 A_{\nu_\tau} H_2^i \tilde{\psi}_{\tau L}^j \tilde{\nu}_{\tau L}^c + h_1 A_\mu H_1^i \tilde{\psi}_{\mu L}^j \tilde{\mu}_L^c - h'_1 A_{\nu_\mu} H_2^i \tilde{\psi}_{\mu L}^j \tilde{\nu}_{\mu L}^c \\ & + h_2 A_e H_1^i \tilde{\psi}_{eL}^j \tilde{e}_L^c - h'_2 A_{\nu_e} H_2^i \tilde{\psi}_{eL}^j \tilde{\nu}_{eL}^c + f_2 A_N H_1^i \tilde{\chi}^{cj} \tilde{N}_L - f'_2 A_E H_2^i \tilde{\chi}^{cj} \tilde{E}_L + \text{H.c.} \} . \end{aligned} \quad (45)$$

Here $M_{\tilde{e}L}, M_{\tilde{\nu}_e}$ etc are the soft masses and A_e, A_{ν_e} etc are the trilinear couplings. The trilinear couplings are complex and we define their phases so that

$$A_e = |A_e| e^{i\alpha_{A_e}} , \quad A_{\nu_e} = |A_{\nu_e}| e^{i\alpha_{A_{\nu_e}}} , \dots . \quad (46)$$

From these terms we construct the scalar mass² matrices [27] which are exhibited in Appendix C.

As discussed in Section 3 and Section 4 the inclusion of the vector like generation brings in new phenomena such as exchange contributions from the W and Z bosons which are otherwise absent. Their inclusion gives an important contribution to the EDM since the W and the Z boson contribution begins to play a role and leads to constructive and destructive interference with the chargino and neutralino exchange contribution. A more detailed description of this phenomenon is given in Section 4.

Appendix B: Interactions that enter in the EDM analysis in the MSSM Extension with a Vector like Multiplet

In this section we discuss the interactions in the mass diagonal basis involving charged leptons, sneutrinos and charginos. Thus we have

$$-\mathcal{L}_{\tau-\tilde{\nu}-\chi^-} = \sum_{i=1}^2 \sum_{j=1}^8 \bar{\tau}_\alpha (C_{\alpha ij}^L P_L + C_{\alpha ij}^R P_R) \tilde{\chi}^{ci} \tilde{\nu}_j + \text{H.c.}, \quad (47)$$

such that

$$C_{\alpha ij}^L = g(-\kappa_\tau U_{i2}^* D_{R1\alpha}^{\tau*} \tilde{D}_{1j}^\nu - \kappa_\mu U_{i2}^* D_{R3\alpha}^{\tau*} \tilde{D}_{5j}^\nu - \kappa_e U_{i2}^* D_{R4\alpha}^{\tau*} \tilde{D}_{7j}^\nu + U_{i1}^* D_{R2\alpha}^{\tau*} \tilde{D}_{4j}^\nu - \kappa_N U_{i2}^* D_{R2\alpha}^{\tau*} \tilde{D}_{2j}^\nu) \quad (48)$$

$$C_{\alpha ij}^R = g(-\kappa_{\nu_\tau} V_{i2} D_{L1\alpha}^{\tau*} \tilde{D}_{3j}^\nu - \kappa_{\nu_\mu} V_{i2} D_{L3\alpha}^{\tau*} \tilde{D}_{6j}^\nu - \kappa_{\nu_e} V_{i2} D_{L4\alpha}^{\tau*} \tilde{D}_{8j}^\nu + V_{i1} D_{L1\alpha}^{\tau*} \tilde{D}_{1j}^\nu + V_{i1} D_{L3\alpha}^{\tau*} \tilde{D}_{5j}^\nu + V_{i1} D_{L4\alpha}^{\tau*} \tilde{D}_{7j}^\nu - \kappa_E V_{i2} D_{L2\alpha}^{\tau*} \tilde{D}_{4j}^\nu), \quad (49)$$

with

$$(\kappa_N, \kappa_\tau, \kappa_\mu, \kappa_e) = \frac{(m_N, m_\tau, m_\mu, m_e)}{\sqrt{2} m_W \cos \beta}, \quad (50)$$

$$(\kappa_E, \kappa_{\nu_\tau}, \kappa_{\nu_\mu}, \kappa_{\nu_e}) = \frac{(m_E, m_{\nu_\tau}, m_{\nu_\mu}, m_{\nu_e})}{\sqrt{2} m_W \sin \beta}. \quad (51)$$

We now discuss the interactions in the mass diagonal basis involving charged leptons, sleptons and neutralinos. Thus we have

$$-\mathcal{L}_{\tau-\tilde{\tau}-\chi^0} = \sum_{i=1}^4 \sum_{j=1}^8 \bar{\tau}_\alpha (C'_{\alpha ij}{}^L P_L + C'_{\alpha ij}{}^R P_R) \tilde{\chi}_i^0 \tilde{\tau}_j + \text{H.c.}, \quad (52)$$

such that

$$C'_{\alpha ij}{}^L = \sqrt{2}(\alpha_{\tau i} D_{R1\alpha}^{\tau*} \tilde{D}_{1j}^\tau - \delta_{Ei} D_{R2\alpha}^{\tau*} \tilde{D}_{2j}^\tau - \gamma_{\tau i} D_{R1\alpha}^{\tau*} \tilde{D}_{3j}^\tau + \beta_{Ei} D_{R2\alpha}^{\tau*} \tilde{D}_{4j}^\tau + \alpha_{\mu i} D_{R3\alpha}^{\tau*} \tilde{D}_{5j}^\tau - \gamma_{\mu i} D_{R3\alpha}^{\tau*} \tilde{D}_{6j}^\tau + \alpha_{ei} D_{R4\alpha}^{\tau*} \tilde{D}_{7j}^\tau - \gamma_{ei} D_{R4\alpha}^{\tau*} \tilde{D}_{8j}^\tau) \quad (53)$$

$$C'_{\alpha ij}{}^R = \sqrt{2}(\beta_{\tau i} D_{L1\alpha}^{\tau*} \tilde{D}_{1j}^\tau - \gamma_{Ei} D_{L2\alpha}^{\tau*} \tilde{D}_{2j}^\tau - \delta_{\tau i} D_{L1\alpha}^{\tau*} \tilde{D}_{3j}^\tau + \alpha_{Ei} D_{L2\alpha}^{\tau*} \tilde{D}_{4j}^\tau + \beta_{\mu i} D_{L3\alpha}^{\tau*} \tilde{D}_{5j}^\tau - \delta_{\mu i} D_{L3\alpha}^{\tau*} \tilde{D}_{6j}^\tau + \beta_{ei} D_{L4\alpha}^{\tau*} \tilde{D}_{7j}^\tau - \delta_{ei} D_{L4\alpha}^{\tau*} \tilde{D}_{8j}^\tau), \quad (54)$$

where

$$\alpha_{Ei} = \frac{gm_E X_{4i}^*}{2m_W \sin \beta}; \quad \beta_{Ei} = eX'_{1i} + \frac{g}{\cos \theta_W} X'_{2i} \left(\frac{1}{2} - \sin^2 \theta_W \right) \quad (55)$$

$$\gamma_{Ei} = eX'_{1i} - \frac{g \sin^2 \theta_W}{\cos \theta_W} X'_{2i}; \quad \delta_{Ei} = -\frac{gm_E X_{4i}}{2m_W \sin \beta} \quad (56)$$

and

$$\alpha_{\tau i} = \frac{gm_\tau X_{3i}}{2m_W \cos \beta}; \quad \alpha_{\mu i} = \frac{gm_\mu X_{3i}}{2m_W \cos \beta}; \quad \alpha_{ei} = \frac{gm_e X_{3i}}{2m_W \cos \beta} \quad (57)$$

$$\delta_{\tau i} = -\frac{gm_\tau X_{3i}^*}{2m_W \cos \beta}; \quad \delta_{\mu i} = -\frac{gm_\mu X_{3i}^*}{2m_W \cos \beta}; \quad \delta_{ei} = -\frac{gm_e X_{3i}^*}{2m_W \cos \beta} \quad (58)$$

and where

$$\beta_{\tau i} = \beta_{\mu i} = \beta_{ei} = -eX'_{1i} + \frac{g}{\cos \theta_W} X'_{2i} \left(-\frac{1}{2} + \sin^2 \theta_W \right) \quad (59)$$

$$\gamma_{\tau i} = \gamma_{\mu i} = \gamma_{ei} = -eX'_{1i} + \frac{g \sin^2 \theta_W}{\cos \theta_W} X'_{2i} \quad (60)$$

Here X' are defined by

$$X'_{1i} = X_{1i} \cos \theta_W + X_{2i} \sin \theta_W \quad (61)$$

$$X'_{2i} = -X_{1i} \sin \theta_W + X_{2i} \cos \theta_W \quad (62)$$

where X diagonalizes the neutralino mass matrix and is defined by Eq.(19).

In addition to the computation of the supersymmetric loop diagrams, we compute the contributions arising from the exchange of the W and Z bosons and the leptons and the mirror leptons in the loops. The relevant interactions needed are given below. For the W boson exchange the interactions that enter are given by

$$-\mathcal{L}_{\tau W \psi} = W_\rho^\dagger \sum_{i=1}^4 \sum_{\alpha=1}^4 \bar{\psi}_i \gamma^\rho [C_{L_{i\alpha}}^W P_L + C_{R_{i\alpha}}^W P_R] \tau_\alpha + \text{H.c.} \quad (63)$$

where

$$C_{L_{i\alpha}}^W = \frac{g}{\sqrt{2}} [D_{L1i}^{\nu*} D_{L1\alpha}^\tau + D_{L3i}^{\nu*} D_{L3\alpha}^\tau + D_{L4i}^{\nu*} D_{L4\alpha}^\tau] \quad (64)$$

$$C_{R_{i\alpha}}^W = \frac{g}{\sqrt{2}} [D_{R2i}^{\nu*} D_{R2\alpha}^\tau] \quad (65)$$

For the Z boson exchange the interactions that enter are given by

$$-\mathcal{L}_{\tau\tau Z} = Z_\rho \sum_{\alpha=1}^4 \sum_{\beta=1}^4 \bar{\tau}_\alpha \gamma^\rho [C_{L\alpha\beta}^Z P_L + C_{R\alpha\beta}^Z P_R] \tau_\beta \quad (66)$$

where

$$C_{L\alpha\beta}^Z = \frac{g}{\cos\theta_W} [x(D_{L\alpha 1}^{\tau\dagger} D_{L1\beta}^\tau + D_{L\alpha 2}^{\tau\dagger} D_{L2\beta}^\tau + D_{L\alpha 3}^{\tau\dagger} D_{L3\beta}^\tau + D_{L\alpha 4}^{\tau\dagger} D_{L4\beta}^\tau) - \frac{1}{2}(D_{L\alpha 1}^{\tau\dagger} D_{L1\beta}^\tau + D_{L\alpha 3}^{\tau\dagger} D_{L3\beta}^\tau + D_{L\alpha 4}^{\tau\dagger} D_{L4\beta}^\tau)] \quad (67)$$

and

$$C_{R\alpha\beta}^Z = \frac{g}{\cos\theta_W} [x(D_{R\alpha 1}^{\tau\dagger} D_{R1\beta}^\tau + D_{R\alpha 2}^{\tau\dagger} D_{R2\beta}^\tau + D_{R\alpha 3}^{\tau\dagger} D_{R3\beta}^\tau + D_{R\alpha 4}^{\tau\dagger} D_{R4\beta}^\tau) - \frac{1}{2}(D_{R\alpha 2}^{\tau\dagger} D_{R2\beta}^\tau)] \quad (68)$$

where $x = \sin^2\theta_W$.

Appendix C : The scalar mass squared matrices

For convenience we collect here all the contributions to the scalar mass² matrices arising from the superpotential. They are given by

$$\mathcal{L}_F^{\text{mass}} = \mathcal{L}_C^{\text{mass}} + \mathcal{L}_N^{\text{mass}} \quad , \quad (69)$$

where $\mathcal{L}_C^{\text{mass}}$ gives the mass terms for the charged sleptons while $\mathcal{L}_N^{\text{mass}}$ gives the mass terms for the sneutrinos. For $\mathcal{L}_C^{\text{mass}}$ we have

$$\begin{aligned} -\mathcal{L}_C^{\text{mass}} = & \left(\frac{v_2^2 |f_2'|^2}{2} + |f_3|^2 + |f_3'|^2 + |f_3''|^2 \right) \tilde{E}_R \tilde{E}_R^* + \left(\frac{v_2^2 |f_2'|^2}{2} + |f_4|^2 + |f_4'|^2 + |f_4''|^2 \right) \tilde{E}_L \tilde{E}_L^* \\ & + \left(\frac{v_1^2 |f_1|^2}{2} + |f_4|^2 \right) \tilde{\tau}_R \tilde{\tau}_R^* + \left(\frac{v_1^2 |f_1|^2}{2} + |f_3|^2 \right) \tilde{\tau}_L \tilde{\tau}_L^* + \left(\frac{v_1^2 |h_1|^2}{2} + |f_4'|^2 \right) \tilde{\mu}_R \tilde{\mu}_R^* \\ & + \left(\frac{v_1^2 |h_1|^2}{2} + |f_3'|^2 \right) \tilde{\mu}_L \tilde{\mu}_L^* + \left(\frac{v_1^2 |h_2|^2}{2} + |f_4''|^2 \right) \tilde{e}_R \tilde{e}_R^* + \left(\frac{v_1^2 |h_2|^2}{2} + |f_3''|^2 \right) \tilde{e}_L \tilde{e}_L^* \\ & + \left\{ -\frac{f_1 \mu^* v_2}{\sqrt{2}} \tilde{\tau}_L \tilde{\tau}_R^* - \frac{h_1 \mu^* v_2}{\sqrt{2}} \tilde{\mu}_L \tilde{\mu}_R^* - \frac{f_2' \mu^* v_1}{\sqrt{2}} \tilde{E}_L \tilde{E}_R^* + \left(\frac{f_2' v_2 f_3^*}{\sqrt{2}} + \frac{f_4 v_1 f_1^*}{\sqrt{2}} \right) \tilde{E}_L \tilde{\tau}_L^* \right. \\ & + \left(\frac{f_4 v_2 f_2'^*}{\sqrt{2}} + \frac{f_1 v_1 f_3^*}{\sqrt{2}} \right) \tilde{E}_R \tilde{\tau}_R^* + \left(\frac{f_3' v_2 f_2'^*}{\sqrt{2}} + \frac{h_1 v_1 f_4^*}{\sqrt{2}} \right) \tilde{E}_L \tilde{\mu}_L^* + \left(\frac{f_2' v_2 f_4^*}{\sqrt{2}} + \frac{f_3' v_1 h_1^*}{\sqrt{2}} \right) \tilde{E}_R \tilde{\mu}_R^* \\ & + \left(\frac{f_3'' v_2 f_2'^*}{\sqrt{2}} + \frac{f_4'' v_1 h_2^*}{\sqrt{2}} \right) \tilde{E}_L \tilde{e}_L^* + \left(\frac{f_4'' v_2 f_2'^*}{\sqrt{2}} + \frac{f_3'' v_1 h_2^*}{\sqrt{2}} \right) \tilde{E}_R \tilde{e}_R^* + f_3' f_3^* \tilde{\mu}_L \tilde{\tau}_L^* + f_4 f_4^* \tilde{\mu}_R \tilde{\tau}_R^* \\ & \left. + f_4 f_4^* \tilde{e}_R \tilde{\tau}_R^* + f_3'' f_3^* \tilde{e}_L \tilde{\tau}_L^* + f_3'' f_3^* \tilde{e}_L \tilde{\mu}_L^* + f_4 f_4^* \tilde{e}_R \tilde{\mu}_R^* - \frac{h_2 \mu^* v_2}{\sqrt{2}} \tilde{e}_L \tilde{e}_R^* + H.c. \right\} \quad (70) \end{aligned}$$

We define the scalar mass squared matrix $M_{\tilde{\tau}}^2$ in the basis $(\tilde{\tau}_L, \tilde{E}_L, \tilde{\tau}_R, \tilde{E}_R, \tilde{\mu}_L, \tilde{\mu}_R, \tilde{e}_L, \tilde{e}_R)$. We label the matrix elements of these as $(M_{\tilde{\tau}}^2)_{ij} = M_{ij}^2$ where the elements of the matrix are given by

$$\begin{aligned}
M_{11}^2 &= \tilde{M}_{\tau L}^2 + \frac{v_1^2 |f_1|^2}{2} + |f_3|^2 - m_Z^2 \cos 2\beta \left(\frac{1}{2} - \sin^2 \theta_W \right), \\
M_{22}^2 &= \tilde{M}_E^2 + \frac{v_2^2 |f_2'|^2}{2} + |f_4|^2 + |f_4'|^2 + |f_4''|^2 + m_Z^2 \cos 2\beta \sin^2 \theta_W, \\
M_{33}^2 &= \tilde{M}_\tau^2 + \frac{v_1^2 |f_1|^2}{2} + |f_4|^2 - m_Z^2 \cos 2\beta \sin^2 \theta_W, \\
M_{44}^2 &= \tilde{M}_\chi^2 + \frac{v_2^2 |f_2'|^2}{2} + |f_3|^2 + |f_3'|^2 + |f_3''|^2 + m_Z^2 \cos 2\beta \left(\frac{1}{2} - \sin^2 \theta_W \right), \\
M_{55}^2 &= \tilde{M}_{\mu L}^2 + \frac{v_1^2 |h_1|^2}{2} + |f_3'|^2 - m_Z^2 \cos 2\beta \left(\frac{1}{2} - \sin^2 \theta_W \right), \\
M_{66}^2 &= \tilde{M}_\mu^2 + \frac{v_1^2 |h_1|^2}{2} + |f_4'|^2 - m_Z^2 \cos 2\beta \sin^2 \theta_W, \\
M_{77}^2 &= \tilde{M}_{eL}^2 + \frac{v_1^2 |h_2|^2}{2} + |f_3''|^2 - m_Z^2 \cos 2\beta \left(\frac{1}{2} - \sin^2 \theta_W \right), \\
M_{88}^2 &= \tilde{M}_e^2 + \frac{v_1^2 |h_2|^2}{2} + |f_4''|^2 - m_Z^2 \cos 2\beta \sin^2 \theta_W.
\end{aligned}$$

$$\begin{aligned}
M_{12}^2 &= M_{21}^{2*} = \frac{v_2 f_2' f_3^*}{\sqrt{2}} + \frac{v_1 f_4 f_1^*}{\sqrt{2}}, M_{13}^2 = M_{31}^{2*} = \frac{f_1^*}{\sqrt{2}} (v_1 A_\tau^* - \mu v_2), M_{14}^2 = M_{41}^{2*} = 0, \\
M_{15}^2 &= M_{51}^{2*} = f_3' f_3^*, M_{16}^{2*} = M_{61}^{2*} = 0, M_{17}^{2*} = M_{71}^{2*} = f_3'' f_3^*, M_{18}^{2*} = M_{81}^{2*} = 0, \\
M_{23}^2 &= M_{32}^{2*} = 0, M_{24}^2 = M_{42}^{2*} = \frac{f_2'^*}{\sqrt{2}} (v_2 A_E^* - \mu v_1), M_{25}^2 = M_{52}^{2*} = \frac{v_2 f_3' f_2'^*}{\sqrt{2}} + \frac{v_1 h_1 f_4^*}{\sqrt{2}}, \\
M_{26}^2 &= M_{62}^{2*} = 0, M_{27}^2 = M_{72}^{2*} = \frac{v_2 f_3'' f_2'^*}{\sqrt{2}} + \frac{v_1 h_1 f_4'^*}{\sqrt{2}}, M_{28}^2 = M_{82}^{2*} = 0, \\
M_{34}^2 &= M_{43}^{2*} = \frac{v_2 f_4 f_2'^*}{\sqrt{2}} + \frac{v_1 f_1 f_3^*}{\sqrt{2}}, M_{35}^2 = M_{53}^{2*} = 0, M_{36}^2 = M_{63}^{2*} = f_4 f_4^*, \\
M_{37}^2 &= M_{73}^{2*} = 0, M_{38}^2 = M_{83}^{2*} = f_4 f_4'^*, \\
M_{45}^2 &= M_{54}^{2*} = 0, M_{46}^2 = M_{64}^{2*} = \frac{v_2 f_2' f_4'^*}{\sqrt{2}} + \frac{v_1 f_3' h_1^*}{\sqrt{2}}, \\
M_{47}^2 &= M_{74}^{2*} = 0, M_{48}^2 = M_{84}^{2*} = \frac{v_2 f_2' f_4''^*}{\sqrt{2}} + \frac{v_1 f_3'' h_2^*}{\sqrt{2}}, \\
M_{56}^2 &= M_{65}^{2*} = \frac{h_1^*}{\sqrt{2}} (v_1 A_\mu^* - \mu v_2), M_{57}^2 = M_{75}^{2*} = f_3'' f_3^*, \\
M_{58}^2 &= M_{85}^{2*} = 0, M_{67}^2 = M_{76}^{2*} = 0, \\
M_{68}^2 &= M_{86}^{2*} = f_4' f_4'^*, M_{78}^2 = M_{87}^{2*} = \frac{h_2^*}{\sqrt{2}} (v_1 A_e^* - \mu v_2).
\end{aligned}$$

We can diagonalize this hermitian mass squared matrix by the unitary transformation

$$\tilde{D}^{\dagger} M_{\tilde{\nu}}^2 \tilde{D}^{\tau} = \text{diag}(M_{\tilde{\nu}_1}^2, M_{\tilde{\nu}_2}^2, M_{\tilde{\nu}_3}^2, M_{\tilde{\nu}_4}^2, M_{\tilde{\nu}_5}^2, M_{\tilde{\nu}_6}^2, M_{\tilde{\nu}_7}^2, M_{\tilde{\nu}_8}^2). \quad (71)$$

For $\mathcal{L}_N^{\text{mass}}$ we have

$$\begin{aligned} -\mathcal{L}_N^{\text{mass}} = & \left(\frac{v_1^2 |f_2|^2}{2} + |f_3|^2 + |f_3'|^2 + |f_3''|^2 \right) \tilde{N}_R \tilde{N}_R^* \\ & + \left(\frac{v_1^2 |f_2|^2}{2} + |f_5|^2 + |f_5'|^2 + |f_5''|^2 \right) \tilde{N}_L \tilde{N}_L^* + \left(\frac{v_2^2 |f_1|^2}{2} + |f_5|^2 \right) \tilde{\nu}_{\tau R} \tilde{\nu}_{\tau R}^* \\ & + \left(\frac{v_2^2 |f_1|^2}{2} + |f_3|^2 \right) \tilde{\nu}_{\tau L} \tilde{\nu}_{\tau L}^* + \left(\frac{v_2^2 |h_1|^2}{2} + |f_3|^2 \right) \tilde{\nu}_{\mu L} \tilde{\nu}_{\mu L}^* + \left(\frac{v_2^2 |h_1|^2}{2} + |f_5|^2 \right) \tilde{\nu}_{\mu R} \tilde{\nu}_{\mu R}^* \\ & + \left(\frac{v_2^2 |h_2|^2}{2} + |f_3|^2 \right) \tilde{\nu}_{eL} \tilde{\nu}_{eL}^* + \left(\frac{v_2^2 |h_2|^2}{2} + |f_5''|^2 \right) \tilde{\nu}_{eR} \tilde{\nu}_{eR}^* \\ & + \left\{ -\frac{f_2 \mu^* v_2}{\sqrt{2}} \tilde{N}_L \tilde{N}_R^* - \frac{f_1 \mu^* v_1}{\sqrt{2}} \tilde{\nu}_{\tau L} \tilde{\nu}_{\tau R}^* - \frac{h_1' \mu^* v_1}{\sqrt{2}} \tilde{\nu}_{\mu L} \tilde{\nu}_{\mu R}^* + \left(\frac{f_5 v_2 f_1^*}{\sqrt{2}} - \frac{f_2 v_1 f_3^*}{\sqrt{2}} \right) \tilde{N}_L \tilde{\nu}_{\tau L}^* \right. \\ & + \left(\frac{f_5 v_1 f_2^*}{\sqrt{2}} - \frac{f_1 v_2 f_3^*}{\sqrt{2}} \right) \tilde{N}_R \tilde{\nu}_{\tau R}^* + \left(\frac{h_1' v_2 f_5^*}{\sqrt{2}} - \frac{f_3' v_1 f_2^*}{\sqrt{2}} \right) \tilde{N}_L \tilde{\nu}_{\mu L}^* + \left(\frac{f_5' v_1 f_2^*}{\sqrt{2}} - \frac{f_3'' v_2 h_2^*}{\sqrt{2}} \right) \tilde{N}_R \tilde{\nu}_{eR}^* \\ & + \left(\frac{h_2' v_2 f_5^*}{\sqrt{2}} - \frac{f_3'' v_1 f_2^*}{\sqrt{2}} \right) \tilde{N}_L \tilde{\nu}_{eL}^* + \left(\frac{f_5' v_1 f_2^*}{\sqrt{2}} - \frac{h_1' v_2 f_3^*}{\sqrt{2}} \right) \tilde{N}_R \tilde{\nu}_{\mu R}^* \\ & \quad + f_3' f_3^* \tilde{\nu}_{\mu L} \tilde{\nu}_{\tau L}^* + f_5 f_5^* \tilde{\nu}_{\mu R} \tilde{\nu}_{\tau R}^* - \frac{h_2' \mu^* v_1}{\sqrt{2}} \tilde{\nu}_{eL} \tilde{\nu}_{eR}^* \\ & \quad \left. + f_3'' f_3^* \tilde{\nu}_{eL} \tilde{\nu}_{\tau L}^* + f_5 f_5''^* \tilde{\nu}_{eR} \tilde{\nu}_{\tau R}^* + f_3' f_3^* \tilde{\nu}_{eL} \tilde{\nu}_{\mu L}^* + f_5' f_5^* \tilde{\nu}_{eR} \tilde{\nu}_{\mu R}^* + H.c. \right\}. \end{aligned}$$

Next we write the mass² matrix in the sneutrino sector the basis $(\tilde{\nu}_{\tau L}, \tilde{N}_L, \tilde{\nu}_{\tau R}, \tilde{N}_R, \tilde{\nu}_{\mu L}, \tilde{\nu}_{\mu R}, \tilde{\nu}_{eL}, \tilde{\nu}_{eR})$. Thus here we denote the sneutrino mass² matrix in the form $(M_{\tilde{\nu}}^2)_{ij} = m_{ij}^2$ where

$$\begin{aligned} m_{11}^2 &= \tilde{M}_{\tau L}^2 + m_{\nu_{\tau}}^2 + |f_3|^2 + \frac{1}{2} m_Z^2 \cos 2\beta, \\ m_{22}^2 &= \tilde{M}_N^2 + m_N^2 + |f_5|^2 + |f_5'|^2 + |f_5''|^2, \\ m_{33}^2 &= \tilde{M}_{\nu_{\tau}}^2 + m_{\nu_{\tau}}^2 + |f_5|^2, \\ m_{44}^2 &= \tilde{M}_{\chi}^2 + m_N^2 + |f_3|^2 + |f_3'|^2 + |f_3''|^2 - \frac{1}{2} m_Z^2 \cos 2\beta, \\ m_{55}^2 &= \tilde{M}_{\mu L}^2 + m_{\nu_{\mu}}^2 + |f_3|^2 + \frac{1}{2} m_Z^2 \cos 2\beta, \\ m_{66}^2 &= \tilde{M}_{\nu_{\mu}}^2 + m_{\nu_{\mu}}^2 + |f_5|^2, \\ m_{77}^2 &= \tilde{M}_{eL}^2 + m_{\nu_e}^2 + |f_3''|^2 + \frac{1}{2} m_Z^2 \cos 2\beta, \\ m_{88}^2 &= \tilde{M}_{\nu_e}^2 + m_{\nu_e}^2 + |f_5''|^2, \end{aligned}$$

$$\begin{aligned}
m_{12}^2 &= m_{21}^{2*} = \frac{v_2 f_5 f_1'^*}{\sqrt{2}} - \frac{v_1 f_2 f_3^*}{\sqrt{2}}, \quad m_{13}^2 = m_{31}^{2*} = \frac{f_1'^*}{\sqrt{2}}(v_2 A_{\nu_\tau}^* - \mu v_1) \\
m_{14}^2 &= m_{41}^{2*} = 0, \quad m_{15}^2 = m_{51}^{2*} = f_3' f_3^*, \quad m_{16}^2 = m_{61}^{2*} = 0, \\
m_{17}^2 &= m_{71}^{2*} = f_3'' f_3^*, \quad m_{18}^2 = m_{81}^{2*} = 0, \\
m_{23}^2 &= m_{32}^{2*} = 0, \quad m_{24}^2 = m_{42}^{2*} = \frac{f_2^*}{\sqrt{2}}(v_1 A_N^* - \mu v_2), \\
m_{25}^2 &= m_{52}^{2*} = -\frac{v_1 f_2^* f_3'}{\sqrt{2}} + \frac{h_1' v_2 f_5'^*}{\sqrt{2}}, \\
m_{26}^2 &= m_{62}^{2*} = 0, \quad m_{27}^2 = m_{72}^{2*} = -\frac{v_1 f_2^* f_3''}{\sqrt{2}} + \frac{h_2' v_2 f_5''^*}{\sqrt{2}} \\
m_{28}^2 &= m_{82}^{2*} = 0, \quad m_{34}^2 = m_{43}^{2*} = \frac{v_1 f_2^* f_5}{\sqrt{2}} - \frac{v_2 f_1' f_3^*}{\sqrt{2}}, \\
m_{35}^2 &= m_{53}^{2*} = 0, \quad m_{36}^2 = m_{63}^{2*} = f_5 f_5'^*, \\
m_{37}^2 &= m_{73}^{2*} = 0, \quad m_{38}^2 = m_{83}^{2*} = f_5 f_5''^*, \\
m_{45}^2 &= m_{54}^{2*} = 0, \quad m_{46}^2 = m_{64}^{2*} = -\frac{h_1^* v_2 f_3'}{\sqrt{2}} + \frac{v_1 f_2 f_5'^*}{\sqrt{2}}, \\
m_{47}^2 &= m_{74}^{2*} = 0, \quad m_{48}^2 = m_{84}^{2*} = \frac{v_1 f_2 f_5''^*}{\sqrt{2}} - \frac{v_2 h_2^* f_3''}{\sqrt{2}}, \\
m_{56}^2 &= m_{65}^{2*} = \frac{h_1^*}{\sqrt{2}}(v_2 A_{\nu_\mu}^* - \mu v_1), \\
m_{57}^2 &= m_{75}^{2*} = f_3'' f_3^*, \quad m_{58}^2 = m_{85}^{2*} = 0, \\
m_{67}^2 &= m_{76}^{2*} = 0, \quad m_{68}^2 = m_{86}^{2*} = f_5' f_5''^*, \\
m_{78}^2 &= m_{87}^{2*} = \frac{h_2^*}{\sqrt{2}}(v_2 A_{\nu_e}^* - \mu v_1). \tag{72}
\end{aligned}$$

We can diagonalize the sneutrino mass square matrix by the unitary transformation

$$\tilde{D}^{\nu\dagger} M_{\tilde{\nu}}^2 \tilde{D}^\nu = \text{diag}(M_{\tilde{\nu}_1}^2, M_{\tilde{\nu}_2}^2, M_{\tilde{\nu}_3}^2, M_{\tilde{\nu}_4}^2, M_{\tilde{\nu}_5}^2, M_{\tilde{\nu}_6}^2, M_{\tilde{\nu}_7}^2, M_{\tilde{\nu}_8}^2). \tag{73}$$

References

- [1] W. Bernreuther and M. Suzuki, Rev. Mod. Phys. **63**, 313 (1991); I.I.Y. Bigi and N. G. Uraltsev, Sov. Phys. JETP **73**, 198 (1991); M. J. Booth, eprint hep-ph/9301293; Gavela, M. B., et al., Phys. Lett. B109, 215 (1982); I. B. Khriplovich and A. R. Zhitnitsky, Phys. Lett. B109, 490 (1982); E. P. Shabalin, Sov. Phys. Usp. **26**, 297 (1983); I. B. Kriplovich and S. K. Lamoureaux, *CP Violation Without Strangeness*, (Springer, 1997).
- [2] T. Ibrahim and P. Nath, Rev. Mod. Phys. **80**, 577 (2008); arXiv:hep-ph/0210251. A. Pilaftsis, hep-ph/9908373; M. Pospelov and A. Ritz, Annals Phys. **318**, 119 (2005) [hep-ph/0504231]; J. Engel, M. J. Ramsey-Musolf and U. van Kolck, Prog. Part. Nucl. Phys. **71**, 21 (2013) [arXiv:1303.2371 [nucl-th]].
- [3] J. Ellis, S. Ferrara, and D. V. Nanopoulos, Phys. Lett. **114B** (1982) 231; W. Buchmuller and D. Wyler, Phys. Lett. B121 (1983) 321; F. del’Aguila, M. B. Gavela, J. A. Grifols and A. Mendez, Phys. Lett. B126 (1983) 71; J. Polchinski and M. B. Wise, Phys. Lett. B125 (1983) 393; E. Franco and M. Mangano, Phys. Lett. B135 (1984) 445.
- [4] P. Nath, Phys. Rev. Lett. **66**, 2565 (1991); Y. Kizukuri and N. Oshimo, Phys. Rev. D **46**, 3025 (1992).
- [5] T. Ibrahim and P. Nath, Phys. Lett. B **418**, 98 (1998) [hep-ph/9707409]; Phys. Rev. D **57**, 478 (1998) [hep-ph/9708456]; Phys. Rev. D **58**, 111301 (1998) [hep-ph/9807501]; T. Falk and K. A. Olive, Phys. Lett. B **439**, 71 (1998) [hep-ph/9806236]; M. Brhlik, G. J. Good and G. L. Kane, Phys. Rev. D **59**, 115004 (1999) [hep-ph/9810457].
- [6] D. McKeen, M. Pospelov and A. Ritz, Phys. Rev. D **87**, no. 11, 113002 (2013) [arXiv:1303.1172 [hep-ph]].
- [7] T. Moroi and M. Nagai, Phys. Lett. B **723**, 107 (2013) [arXiv:1303.0668 [hep-ph]].
- [8] W. Altmannshofer, R. Harnik and J. Zupan, JHEP **1311**, 202 (2013) [arXiv:1308.3653 [hep-ph]].
- [9] M. Dhuria and A. Misra, arXiv:1308.3233 [hep-ph].
- [10] J. Baron *et al.* [ACME Collaboration], Science **343**, no. 6168, 269 (2014) [arXiv:1310.7534 [physics.atom-ph]].

- [11] J. Beringer et al. (Particle Data Group), Phys. Rev. D **86**, 010001 (2012).
- [12] Y. Sakemi *et al.*, J. Phys. Conf. Ser. **302** (2011) 012051.
- [13] D. M. Kara *et al.*, New J. Phys. **14** (2012) 103051.
- [14] D. Kawall, J. Phys. Conf. Ser. **295** (2011) 012031.
- [15] J. D. Wells, Phys. Rev. D **71**, 015013 (2005) [hep-ph/0411041].
- [16] T. Ibrahim and P. Nath, Phys. Rev. D **62**, 095001 (2000) [hep-ph/0004098]; R. L. Arnowitt and P. Nath, Phys. Rev. D **49**, 1479 (1994) [hep-ph/9309252]; For a review see, P. Nath and P. Fileviez Perez, Phys. Rept. **441**, 191 (2007) [hep-ph/0601023].
- [17] H. Georgi, Nucl. Phys. B **156**, 126 (1979); F. Wilczek and A. Zee, Phys. Rev. D **25**, 553 (1982); J. Maalampi, J.T. Peltoniemi, and M. Roos, PLB **220**, 441(1989); J. Maalampi and M. Roos, Phys. Rept. **186**, 53 (1990); K. S. Babu, I. Gogoladze, P. Nath and R. M. Syed, Phys. Rev. D **72**, 095011 (2005) [hep-ph/0506312]; Phys. Rev. D **74**, 075004 (2006), [arXiv:hep-ph/0607244]; Phys. Rev. D **85**, 075002 (2012) [arXiv:1112.5387 [hep-ph]]; P. Nath and R. M. Syed, Phys. Rev. D **81**, 037701 (2010).
- [18] K. S. Babu, I. Gogoladze, M. U. Rehman and Q. Shafi, Phys. Rev. D **78**, 055017 (2008).
- [19] C. Liu, Phys. Rev. D **80**, 035004 (2009) [arXiv:0907.3011 [hep-ph]].
- [20] S. P. Martin, Phys. Rev. D **81**, 035004 (2010) [arXiv:0910.2732 [hep-ph]].
- [21] A. Aboubrahim, T. Ibrahim, A. Itani and P. Nath, Phys. Rev. D **89**, 055009 (2014) [arXiv:1312.2505 [hep-ph]].
- [22] A. Aboubrahim, T. Ibrahim and P. Nath, Phys. Rev. D **88**, 013019 (2013) [arXiv:1306.2275 [hep-ph]].
- [23] T. Ibrahim and P. Nath, Phys. Rev. D **78**, 075013 (2008) [arXiv:0806.3880 [hep-ph]].
- [24] T. Ibrahim and P. Nath, Phys. Rev. D **81**, 033007 (2010) [arXiv:1001.0231 [hep-ph]].
- [25] T. Ibrahim and P. Nath, Phys. Rev. D **84**, 015003 (2011) [arXiv:1104.3851 [hep-ph]].
- [26] T. Ibrahim and P. Nath, Phys. Rev. D **82**, 055001 (2010) [arXiv:1007.0432 [hep-ph]].
- [27] T. Ibrahim and P. Nath, Phys. Rev. D **87**, 015030 (2013) [arXiv:1211.0622 [hep-ph]].

- [28] T. Ibrahim and P. Nath, Nucl. Phys. Proc. Suppl. **200-202**, 161 (2010) [arXiv:0910.1303 [hep-ph]].
- [29] P. A. R. Ade *et al.* [Planck Collaboration], arXiv:1303.5062 [astro-ph.CO].
- [30] T. Schwetz, M. A. Tortola and J. W. F. Valle, New J. Phys. **10**, 113011 (2008) [arXiv:0808.2016 [hep-ph]]. See also M. C. Gonzalez-Garcia, M. Maltoni, J. Salvado and T. Schwetz, JHEP **1212**, 123 (2012) [arXiv:1209.3023 [hep-ph]].